Atmospheric Oxidation Mechanism of Methyl Pivalate, $(CH_3)_3CC(O)OCH_3$

T. J. Wallington*

Ford Motor Company, SRL-3083, Dearborn, Michigan 48121-2053

Y. Ninomiya, M. Mashino, and M. Kawasaki

Department of Molecular Engineering, Kyoto University, Kyoto 606-8501, Japan

V. L. Orkin, R. E. Huie, and M. J. Kurylo

Physical and Chemical Properties Division, National Institute of Standards and Technology, Gaithersburg, Maryland 20899-8381

W. P. L. Carter, D. Luo, and I. L. Malkina

CE-CERT, University of California, Riverside, California 92521

Received: January 26, 2001; In Final Form: May 7, 2001

Flash photolysis−resonance fluorescence techniques were used to measure the rate constant for the reaction of OH radicals with methyl pivalate, $(CH_3)_3CC(O)OCH_3$ over the temperature range 250−370 K. The rate constant exhibited a weak temperature dependence, increasing at both low and high temperature from a minimum value of approximately 1.2×10^{-12} cm^3 molecule^{-1} s^{-1} near room temperature. The UV absorption spectrum of methyl pivalate was measured between 160 and 500 nm at room temperature. Smog chamber/FTIR techniques were used to study the Cl atom and OH radical initiated oxidation of $(CH_3)_3CC(O)OCH_3$ in the presence of NO_x in 700 Torr of N_2/O_2 diluent at 296 K. Relative rate techniques were used to measure $k(Cl+(CH_3)_3CC(O)OCH_3) = (4.1 \pm 0.5) \times 10^{-11}$, $k(Cl+(CH_3)_3CC(O)OCH_2Cl) = (1.8 \pm 0.3) \times 10^{-11}$, and $k(Cl+(CH_3)_3CC(O)OC(O)OH) = (1.7 \pm 0.2) \times 10^{-11}$ cm^3 molecule^{-1} s^{-1}. The reaction of Cl atoms with $(CH_3)_3CC(O)OCH_3$ was found to proceed (11 ± 3) % via H-abstraction at the $-OCH_3$ site. The Cl atom initiated oxidation of $(CH_3)_3CC(O)OCH_3$ in the presence of 15−600 Torr of O_2 and 10−30 mTorr of NO_x in 700 Torr total pressure of N_2 diluent at 296 K gives HCHO, CO, acetone, CO_2, and $CH_3OC(O)O_2NO_2$ products. OH radical initiated oxidation of $(CH_3)_3CC(O)OCH_3$ in air produces acetone in a yield of 51 ± 6%. Environmental chamber experiments were performed to quantify the effect of methyl pivalate on ozone formation under simulated atmospheric conditions. An expression representing the atmospheric oxidation mechanism of methyl pivalate in computer models of atmospheric chemistry is recommended.

1. Introduction

Industry consumes multibillion pound quantities of solvents each year in a variety of applications including coatings, inks, adhesives, consumer products, and chemical processing. Regulations that encourage the reduction of solvent emissions are leading manufacturers to consider chemicals which have lower environmental impact. The concept of relative reactivity is being actively pursued for use in formulated products. Methyl pivalate (2,2-dimethylpropanoic acid methyl ester, $(CH_3)_3CC(O)OCH_3$) is under consideration for use in a broad number of applications as a solvent with low ozone formation potential. Methyl pivalate is a volatile compound (bp 101 °C) and may be released into the atmosphere during its use. Prior to large scale production and use of methyl pivalate its reactivity in the atmosphere needs to be established.

The atmospheric oxidation of methyl pivalate is initiated by reaction with OH radicals

$$(CH_3)_3CC(O)OCH_3 + OH \rightarrow (CH_3)_3CC(O)OCH_2\bullet + H_2O \quad (1a)$$

$$(CH_3)_3CC(O)OCH_3 + OH \rightarrow \bullet CH_2(CH_3)_2CC(O)OCH_3 + H_2O \quad (1b)$$

Under atmospheric conditions, the alkyl radicals produced in reaction 1 react with oxygen to give peroxy radicals

$$(CH_3)_3CC(O)OCH_2\bullet + O_2 \rightarrow (CH_3)_3CC(O)OCH_2O_2\bullet \quad (2)$$

$$\bullet CH_2(CH_3)_2CC(O)OCH_3 + O_2 \rightarrow \bullet O_2CH_2(CH_3)_2CC(O)OCH_3 \quad (3)$$

Peroxy radicals react with NO, NO_2, HO_2, and other peroxy radicals in the atmosphere.[1] Reaction with NO_x dominates in polluted air masses. Accurate assessment of the environmental impact of methyl pivalate requires detailed knowledge of its atmospheric chemistry. Unfortunately, there is little available information concerning the atmospheric oxidation mechanism of this compound. To remedy this situation, we report herein the results of a collaborative investigation of the atmospheric chemistry of methyl pivalate.

The investigation comprised of five main elements. First, measurement of the kinetics of the reaction of OH radicals with methyl pivalate. Second, measurement of the UV−visible absorption spectrum of methyl pivalate. Third, determination of the products of the Cl atom and OH radical initiated oxidation of methyl pivalate in air. Fourth, quantification of the impact of methyl pivalate on ozone formation in environmental chamber experiments. Fifth, construction and validation of a detailed mechanism of the atmospheric oxidation mechanism of methyl pivalate.

* To whom correspondence should be addressed. Email: twalling@ford.com

10.1021/jp010308s CCC: $20.00
Published on Web 07/04/2001

2. Experimental Section

The experimental systems used have been described previously.[2,3,4,5−9]

2.1 Flash Photolysis Resonance Fluorescence and UV Absorption Systems at NIST. A flash photolysis−resonance fluorescence (FP−RF) apparatus was used to measure k_1 over the temperature range 250−370 K. The reaction cell was a 60 cm^3 Pyrex sphere thermostated (±1 K) with a fluid circulated through its outer jacket. Dry argon, argon bubbled through water thermostated at 276 K, and a reactant/argon mixture were premixed and flowed through the reaction cell at a total flow rate of ca. 1.4 $cm^3\ s^{-1}$, STP. Flow rates of both argon and H_2O/argon were measured to an accuracy of better than 1% using calibrated mass flow meters. Two different methods were used to measure the flow of methyl pivalate/argon mixtures into the reactor: a mass flow meter (calibration accuracy better than 1%) and direct measurement of the rate of pressure change in a calibrated volume. Different methyl pivalate/argon mixtures (0.05% to 1%) were used to verify that the dilution process did not introduce any systematic error into the rate constant measurement. UV analysis was used to check the composition and stability of methyl pivalate/argon mixtures prepared manometrically in the glass bulbs. Methyl pivalate concentrations determined by UV analysis and calculated from reagent pressures agreed to within 1−2%. The total pressure in the reactor was typically (100.0 ± 0.1) Torr, with a water vapor component of approximately 0.07%. The pressure in the reactor was measured using a MKS Baratron manometer with an absolute accuracy of better than 0.5%. We estimate that the overall systematic uncertainty associated with measurements of the reactant concentration does not exceed 4%. Hydroxyl radicals were produced by the pulsed photolysis (2.5 Hz repetition rate) of H_2O using a xenon flash lamp focused into the reactor. OH radicals were monitored using their resonance fluorescence near 308 nm excited by a microwave discharge resonance lamp focused into the reactor center. The resonance fluorescence signal was recorded on a computer based multichannel scaler (time channel width 100 μs) as a summation of 1000−8000 consecutive flashes. The radical decay signal at each reactant concentration was analyzed as described by Orkin et al.[2] to obtain a first-order decay rate (τ^{-1}_{MP}).

The absorption spectrum of $(CH_3)_3CC(O)OCH_3$ was measured over the wavelength range 160−300 nm at 295 ± 1 K using the single beam apparatus described elsewhere.[3] The complete absorption spectrum was constructed from data taken over several overlapping wavelength ranges for methyl pivalate pressure between 0.1 and 20 Torr (13 Pa − 2.7 kPa) inside the 16.9 ± 0.05 cm absorption cell. The absorption spectrum of the liquid methyl pivalate was also recorded over the wavelength range of 240−500 nm using a Varian Cary double beam spectrophotometer.

Methyl pivalate, $(CH_3)_3CC(O)OCH_3$, was obtained from Aldrich Chemical Co. at a stated purity >99.6% and was subjected to repeated freeze−pump−thaw cycles before use. GC analysis confirmed that the sample was free of impurities.

2.2 FTIR−Smog Chamber System at Ford. All experiments were performed in a 140-liter Pyrex reactor interfaced to a Mattson Sirus 100 FTIR spectrometer.[4] The reactor was surrounded by 22 fluorescent blacklamps (GE F15T8-BL) used to photochemically initiate the experiments. The oxidation of $(CH_3)_3CC(O)OCH_3$ was initiated by reaction with Cl atoms or OH radicals generated by photolysis of molecular chlorine, or methyl nitrite, in 700 Torr of O_2/N_2 diluent at 296 ± 2 K

$$Cl_2 + h\nu \rightarrow 2\ Cl \quad (4)$$

$$Cl + (CH_3)_3CC(O)OCH_3 \rightarrow \text{products} \quad (5)$$

$$CH_3ONO + h\nu \rightarrow CH_3O + NO \quad (6)$$

$$CH_3O + O_2 \rightarrow HCHO + HO_2 \quad (7)$$

$$HO_2 + NO \rightarrow OH + NO_2 \quad (8)$$

$$OH + (CH_3)_3CC(O)OCH_3 \rightarrow \text{products} \quad (1)$$

Loss of $(CH_3)_3CC(O)OCH_3$ and formation of products were monitored by Fourier transform infrared spectroscopy using an infrared path length of 28 m, and a resolution of 0.25 cm^{-1}. Infrared spectra were derived from 32 co-added interferograms.

Calibration of $(CH_3)_3CC(O)OCH_2Cl$, $CH_3C(O)CH_3$, HCHO, CO, and CO_2 reference spectra was achieved by expanding known volumes of these compounds into the chamber. Ultrahigh purity N_2, O_2, and air diluent gases were obtained from Michigan Airgas Corp. All other reagents were obtained from Aldrich Chemical Co. at purities >99%.

In smog chamber experiments, unwanted loss of reactants and products via photolysis, dark chemistry, and wall reactions have to be considered. Control experiments were thus performed to check for such unwanted losses of $(CH_3)_3CC(O)OCH_3$, $(CH_3)_3CC(O)OCH_2Cl$, $(CH_3)_3CC(O)OC(O)OH$, $CH_3C(O)CH_3$, HCHO, CO, and CO_2. No loss (<2%) was observed when these compounds were left to stand in the chamber in the dark for 10 min and then irradiated using the output from the UV fluorescent lamps for 10 min. Photolysis and deposition on the chamber-walls are not important.

2.3 Ozone Reactivity Environmental Chamber Experiments at CE-CERT. Environmental chamber experiments were performed to assess the ability of the chemical mechanism to predict the effects of methyl pivalate on ozone formation and other measures of reactivity under simulated atmospheric conditions. Experiments consisted of the simultaneous irradiation of two mixtures in a dual-reactor environmental chamber at 297 ± 1 K. One reactor contained a reactive organic gas (ROG)−NO_x−air mixture "base case" representing a polluted urban atmosphere. The other reactor contained the same mixture but with varying amounts of methyl pivalate added. Three different base case ROG−NO_x mixtures were employed.

First, the "Mini-Surrogate" base case consisting of a simple 3-component ROG mixture at relatively low ROG/NO_x levels where O_3 formation is most sensitive to VOC levels. This mixture provides a sensitive test of the effect of methyl pivalate on overall radical levels.[5,6] The "Mini-Surrogate" is a mixture of NO (0.30), NO_2 (0.10), *n*-hexane (0.50), ethene (0.85), and *m*-xylene (0.13). Values in parentheses indicate the initial concentrations in ppm (at 300 K and 740 Torr pressure 1 ppm = 2.4×10^{13} molecules cm^{-3}).

Second, the "High NO_x Full Surrogate" base case, which employed a more realistic 8-component ROG mixture, also at relatively low ROG/NO_x ratios where O_3 formation is sensitive to VOCs was employed. This base case mixture is a closer approximation of atmospheric conditions in terms of O_3 impacts of added methyl pivalate.[6] The initial mixture (average concentrations in ppm) was the following: NO (0.27), NO_2 (0.05), *n*-butane (0.41), *n*-octane (0.10), ethene (0.07), propene (0.06), *trans*-2-butene (0.06), toluene (0.09), *m*-xylene (0.09), and formaldehyde (0.10).

Third, the "Low NO_x Full Surrogate" base case which employed the same 8-component ROG mixture as the "High

NO_x Full Surrogate" but with reduced NO and NO_2 concentrations of 0.07 and 0.04 ppm, respectively, was employed. This mixture provides a test of the mechanism under lower NO_x conditions.[6] In addition to the experiments with methyl pivalate, a series of control and characterization experiments were carried out to characterize the conditions of the experiments for mechanism evaluation.[7,8]

All experiments were performed using the CE-CERT "Dividable Teflon Chamber" (DTC) consisting of two ~6000-liter 2-mil heat-sealed FEP Teflon reaction bags fitted inside an 8′ × 8′ × 8′ framework with two diametrically opposed banks of 32 Sylvania 40-W BL black lights. The reaction bags were interconnected with ports containing fans to exchange the contents of the bags. Separate fans were employed to mix the contents within each chamber. The ports were closed and all fans were turned off during the irradiations. Pure dry air was produced using an Aadco air purification system and used to purge the chamber overnight (for 6−9 h) between experiments. The base case reactants were injected into both reactors and mixed as described previously,[5,9] with the methyl pivalate added to one side after the ports connecting the reactors were closed. The irradiations proceeded for 6 h.

The light intensity was measured by NO_2 actinometry.[9,10] The average NO_2 photolysis rate was 0.162 min^{-1}. The flexible design of the reaction bags ensures that dilution due to sampling was negligible. Ozone and nitrogen oxides were monitored continuously using commercially available analyzers. Organic reactants were monitored using gas chromatography with flame ionization detection. Formaldehyde was monitored using a diffusion scrubber method.[9,11,12]

Two measures of the reactivity of methyl pivalate were considered when evaluating the ability of the chemical mechanism to simulate the environmental chamber experiments with this compound. The first measure of reactivity used was the change in the quantity $([O_3]_t - [NO]_t) - ([O_3]_0 - [NO]_0)$, or $\Delta([O_3] - [NO])$. This provides a direct measure of the chemical processes responsible for ozone formation that is useful even when O_3 is suppressed by high NO levels.[13,14,15] The incremental reactivity of methyl pivalate relative to this quantity is given by

$$\mathrm{IR}[\Delta([O_3] - [NO])_t] = \frac{\Delta([O_3] - [NO])_t^{\mathrm{Test}} - \Delta([O_3] - [NO])_t^{\mathrm{Base}}}{[\text{methyl pivalate}]_0} \quad \text{(I)}$$

where $\Delta([O_3] - [NO])_t^{\mathrm{Test}}$ is the change in $([O_3] - [NO])$ measured at time t in an experiment where methyl pivalate was added to the base case, $\Delta([O_3] - [NO])_t^{\mathrm{Base}}$ is the change in the corresponding base case run, and $[\text{methyl pivalate}]_0$ is the amount of methyl pivalate added. An estimated uncertainty for $\mathrm{IR}[\Delta([O_3] - [NO])]$ was derived by assuming an ~3% uncertainty or imprecision in the measurements of O_3 and NO concentrations.

The second measure of reactivity used for mechanism evaluation was the effect of added methyl pivalate on the integrated hydroxyl radical concentration (IntOH). It is important that the mechanism be able to predict this quantity because the effect of methyl pivalate on OH radical levels will affect O_3 formation rates from all other reactive compounds present.[6,7,8,16,18] It was determined from the rate of consumption of *m*-xylene in the experiments (*m*-xylene is consumed only by reaction OH radicals) using

$$\mathrm{IntOH}_t = \frac{\ln([\text{xylene}]_0/[\text{xylene}]_t)}{k\mathrm{OH}^{\text{xylene}}} \quad \text{(II)}$$

$[\text{xylene}]_0$ and $[\text{xylene}]_t$ are the initial and time = t concentrations of *m*-xylene, and $k\mathrm{OH}^{\text{xylene}}$ is the rate constant for reaction of OH radicals with xylene (2.36×10^{-11} cm^3 $molecule^{-1}$ s^{-1}.[17]). The effect of methyl pivalate on the OH radical concentration is measured by its IntOH incremental reactivity, which is defined as

$$\mathrm{IR}[\mathrm{IntOH}]_t = \frac{\mathrm{IntOH}_t^{\mathrm{Test}} - \mathrm{IntOH}_t^{\mathrm{Base}}}{[\text{methyl pivalate}]_0} \quad \text{(III)}$$

$\mathrm{IntOH}^{\mathrm{Test}}$ and $\mathrm{IntOH}^{\mathrm{Base}}$ are the IntOH values measured at time t in the added methyl pivalate and base case experiment, respectively. The uncertainties in IntOH and IR[IntOH] were estimated by assuming an ~2% imprecision in the measurements of the *m*-xylene concentrations.

2.4 Environmental Chamber Modeling Methods. The ozone reactivity environmental chamber experiments were modeled using the SAPRC-99 chemical mechanism.[18] The atmospheric oxidation mechanism for methyl pivalate developed herein reflects improvements in our understanding of the chemistry of this species and supersedes that given recently by Carter.[18] The chemistry of methyl pivalate and all organic compounds present initially in the base case experiments was represented explicitly in the mechanism. Higher molecular weight organic products were represented using lumped model species.

Model simulations of environmental chamber experiments require appropriate representations of chamber effects such as the chamber radical source.[19] These effects were represented as discussed previously.[8,9] Initial reactant concentrations used in the simulations were those measured experimentally. Photolysis rates were calculated using the measured NO_2 photolysis rate, the blacklight spectrum,[9] and absorption cross sections and quantum yields given by Carter.[18]

3. Results

3.1 Absolute Rate Study of k(OH+Methyl Pivalate). OH resonance fluorescence decays were analyzed to obtain pseudo first-order decay rates for each methyl pivalate concentration.[2] Figure 1 shows a plot of the pseudo first-order decay rates vs methyl pivalate concentration at 272 K. Linear least-squares analysis of the data in Figure 1 gives $k_1 = (1.24 \pm 0.02) \times 10^{-12}$ cm^3 $molecule^{-1}$ s^{-1}. Results obtained at other temperatures are listed in Table 1, quoted uncertainties represent the 95% confidence intervals associated with the statistical analysis. As discussed in section 2.1, we estimate that possible systematic errors associated with measurement of the methyl pivalate concentration contribute an additional 4% uncertainty. The measured rate constants are plotted in Arrhenius form in Figure 2.

The methyl pivalate sample had a stated purity >99.6%. Even if present at a level of 0.4%, the impurities that are most likely to be present in the methyl pivalate sample could not result in any appreciable overestimation of the measured rate constant. For example, the rate constant for the reaction between OH and methanol is 8.9×10^{-13} $cm^3molecule^{-1}s^{-1}$ at $T = 298$ K.[20] This would result in a 0.3% error in the rate constant if the total 0.4% impurity level is assigned to methanol. There is no information available on reactivity of pivalic acid toward OH. Nevertheless, we can consider the reactivity of other organic

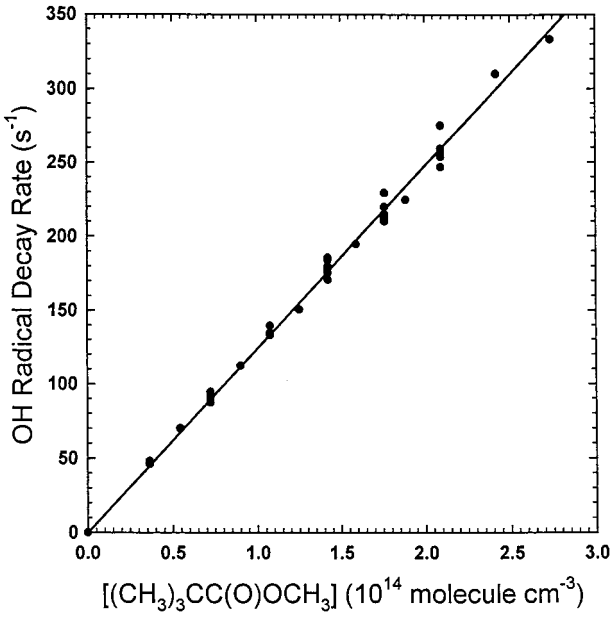

Figure 1. Pseudo first-order OH decay rate vs methyl pivalate concentration from experiments at 272 K (40 data points).

TABLE 1: Kinetic Data for the Reaction of OH with $(CH_3)_3C-C(O)-O-CH_3$[a]

T, K	$[(CH_3)_3CC(O)OCH_3]$ range, (10^{14} molecule cm^{-3})	$k_1 \times 10^{12}$ (cm^{3}molecule^{-1}s^{-1})
250	0.099−3.06	1.37 ± 0.03
272	0.364−2.09	1.24 ± 0.02
298	0.167−3.79	1.20 ± 0.03
330	0.301−2.88	1.22 ± 0.02
370	0.135−2.56	1.38 ± 0.03

a)Error bars are 95% confidence intervals from the statistical analysis and do not include potential systematic errors, see text for details.

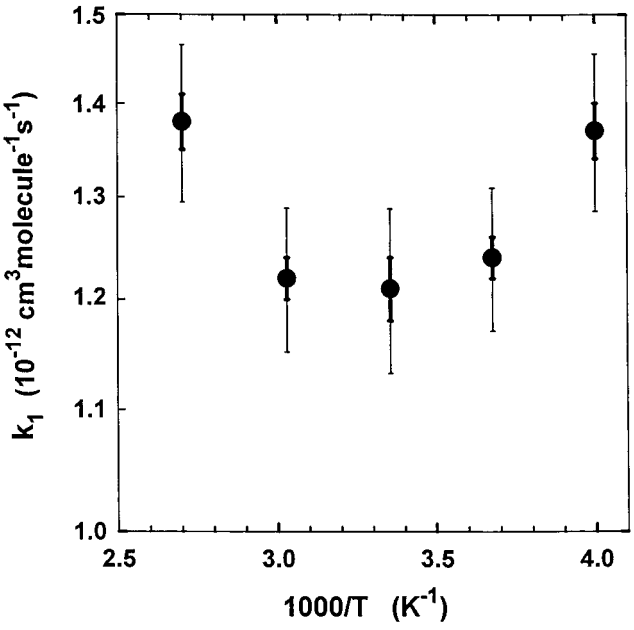

Figure 2. Arrhenius plot showing the average values obtained for k_1 at each temperature. The thick error bars at each temperature represent the 95% confidence intervals from statistical analysis only. The fine lines represent total errors that include the estimated systematic error of 4%.

acids. The rate constant for reaction of OH with the structurally similar acid, 2-methylpropanoic acid, $(CH_3)_2CHCOOH$, is 2×10^{-12} cm^{3}molecule^{-1}s^{-1} at $T = 298$ K.[21] At 0.4% impurity level, this would result in less than 0.7% error.

OH radicals can react with the radical products of reaction 1 or with the relatively stable products that can accumulate in the reactor because of the multiflash experimental procedure. As a check on these possibilities, experiments were performed using different flash energies to increase the initial OH concentration and, hence, the concentrations of radicals and stable products. Varying the flash energy by a factor of 9 resulted in variations in the measured rate constant of less than 6%. Nevertheless, the results presented in Table 1 and Figures 1 and 2 were obtained only from experiments performed at the lowest flash energy of 0.24 J to minimize any possible error due to "secondary chemistry".

There are no other studies of reaction 1 to compare with the present results. Nevertheless several observations can be made. First, the rate constant obtained at room temperature for methyl pivalate is the same as measured for 3,3-dimethyl-2-butanone, $(CH_3)_3CC(O)CH_3$, 1.2×10^{-12} cm^{3}molecule^{-1}s^{-1}.[22] Second, it is noticeably higher than the rate constant measured for dimethyl carbonate, $CH_3OC(O)OCH_3$, 0.31×10^{-12},[23] methyl acetate, $CH_3OC(O)CH_3$, 0.33×10^{-12},[24,25] and acetone, $CH_3C(O)CH_3$, 0.18×10^{-12} cm^{3}molecule^{-1}s^{-1}.[26,27] These comparisons suggest that the majority of the reaction occurs at the $-C(O)C(CH_3)_3$ site of methyl pivalate (reaction 1b). This conclusion is consistent with the results of the product studies presented in section 3.6.

Figure 2 shows the unusual temperature dependence for reaction 1, with a slight increase in the rate constant as the temperature is either raised or lowered about room temperature. These changes lie outside of the statistical uncertainty of the individual points. This behavior is identical to that observed for dimethyl carbonate, $CH_3OC(O)OCH_3$,[23] and methyl acetate, $CH_3OC(O)CH_3$.[24,25] Such a temperature dependence may indicate the existence of two reaction pathways, direct hydrogen abstraction at higher temperature and a reaction proceeding via an addition complex formation at lower temperature. For the three above cases, the reactants contain the $CH_3OC(O)$ group. However, recent studies[26,27] demonstrated similar non-Arrhenius behavior for acetone, $CH_3C(O)CH_3$ as well. These observations support the hypothesis that the C═O group in the reactant is associated with the reaction pathway involving complex formation. On the basis of the observed temperature dependencies one can conclude that both reaction pathways are comparable near room temperature for all three molecules, methyl pivalate, dimethyl carbonate, methyl acetate. However, the fact that methyl pivalate is four times more reactive than dimethyl carbonate suggests that OH forms a transition complex with the *tert*-butyl rather than with methyl side of methyl pivalate, as discussed above:

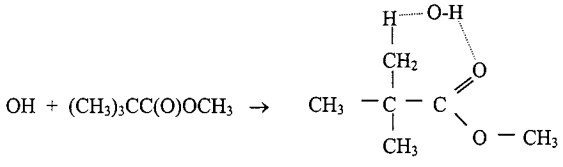

3.2 UV Absorption Spectrum of Methyl Pivalate. Figure 3 shows the gas-phase UV absorption spectrum obtained over the spectral range 160−300 nm. The position of the long wavelength absorption band corresponds reasonably to those of methyl and ethyl acetate.[28] Analysis of the absorption spectra of liquid samples resulted in the absorption cross sections of methyl pivalate smaller than 10^{-22} cm^2/molecule at wavelengths

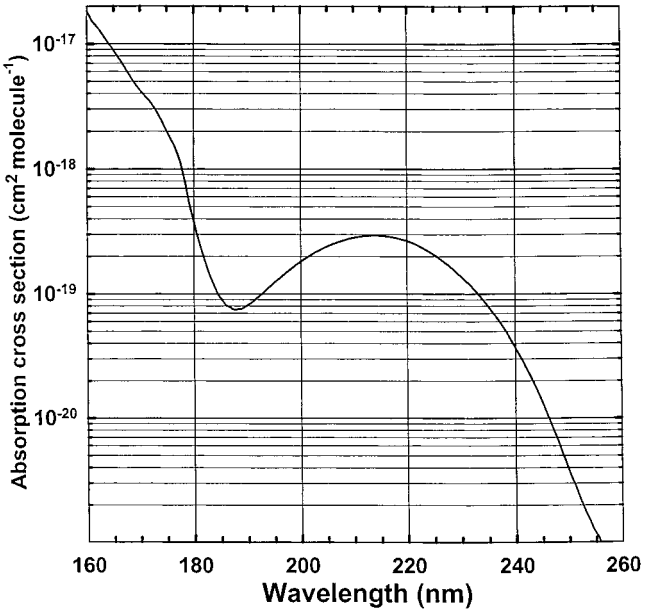

Figure 3. Ultraviolet absorption spectrum (base e) of gaseous methyl pivalate at 295 K.

longer than 280 nm. In contrast to ketones and aldehydes,[28] methyl pivalate does not absorb radiation at wavelengths exceeding 290 nm and will not undergo photolysis in the troposphere.

3.3 Relative Rate Studies of the Reactions of Cl Atoms with $(CH_3)_3CC(O)OCH_3$, $(CH_3)_3CC(O)OCH_2Cl$, and $(CH_3)_3CC(O)OC(O)OH$. Prior to investigating the atmospheric oxidation products of methyl pivalate, relative rate experiments were performed in which the kinetics of reactions (9), (10), and (11) were measured relative to (12) and (13). Initial concentrations used were 7−30 mTorr $(CH_3)_3CC(O)OCH_3$, 5−6 mTorr $(CH_3)_3CC(O)OCH_2Cl$, 4−5 mTorr $(CH_3)_3CC(O)OC(O)OH$, 4−5 mTorr of C_2H_4, 30−53 mTorr of C_2H_5Cl, and 75−240 mTorr of Cl_2, in 700 Torr of air, or N_2, diluent.

$$Cl + (CH_3)_3CC(O)OCH_3 \rightarrow \text{products} \quad (9)$$

$$Cl + (CH_3)_3CC(O)OCH_2Cl \rightarrow \text{products} \quad (10)$$

$$Cl + (CH_3)_3CC(O)OC(O)OH \rightarrow \text{products} \quad (11)$$

$$Cl + C_2H_4 \rightarrow \text{products} \quad (12)$$

$$Cl + C_2H_5Cl \rightarrow \text{products} \quad (13)$$

The observed losses of $(CH_3)_3CC(O)OCH_3$ (MP), $(CH_3)_3CC(O)OCH_2Cl$ (MP−Cl), and $(CH_3)_3CC(O)OC(O)OH$ (PA) vs those of reference compounds in the presence of Cl atoms are shown in Figure 4. Indistinguishable results were obtained in N_2 and air diluent. Linear least-squares analysis of the data in Figure 4, give the rate constant ratios listed in Table 2. Values of k_9, k_{10}, and k_{11} were derived using $k_{12} = 9.29 \times 10^{-11}$ [29] and $k_{13} = 8.04 \times 10^{-12}$.[30] We choose to cite final values of k_9, k_{10}, and k_{11} which are the averages of the individual determinations given in Table 2 with uncertainties which encompass the extremes of the individual determinations. Hence, $k_9 = (4.1 \pm 0.5) \times 10^{-11}$, $k_{10} = (1.8 \pm 0.3) \times 10^{-11}$, and $k_{11} = (1.7 \pm 0.2) \times 10^{-11}$ cm^3 molecule^{-1} s^{-1}.

3.4 Mechanism of the Reaction of Cl Atoms with $(CH_3)_3CC(O)OCH_3$. To investigate the mechanism of reaction 9, experiments were performed using UV irradiation of $(CH_3)_3CC(O)OCH_3/Cl_2/N_2$ mixtures. Initial concentrations were 0.5 Torr of Cl_2 and 15 mTorr $(CH_3)_3CC(O)OCH_3$ in 700 Torr of N_2. Reaction mixtures were subjected to 3−5 successive irradiations each having a duration of 0.5−1 s. In such experiments, $CH_2Cl(CH_3)_2CC(O)OCH_3$ and $(CH_3)_3CC(O)OCH_2Cl$ are produced by the following sequence of chain reactions

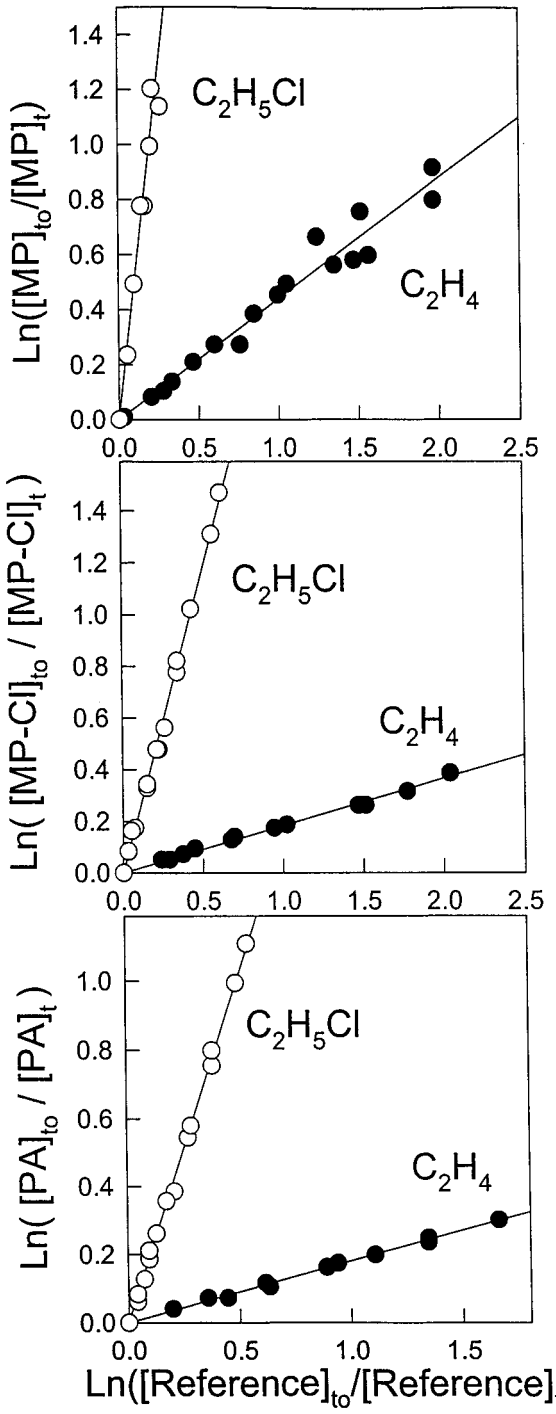

Figure 4. Loss of methyl pivalate (MP), chloromethyl pivalate (MP−Cl), and pivalic acid (PA) vs C_2H_5Cl (○) and C_2H_4 (●) in the presence of Cl atoms in 700 Torr of N_2 at 296 K.

$$Cl + (CH_3)_3CC(O)OCH_3 \rightarrow (CH_3)_3CC(O)OCH_2\bullet + HCl \quad (9a)$$

$$Cl + (CH_3)_3CC(O)OCH_3 \rightarrow \bullet CH_2(CH_3)_2CC(O)OCH_3 + HCl \quad (9b)$$

TABLE 2: Kinetic Data for Reactions Involving Cl Atoms Measured at 296 ± 2 K

	$(CH_3)_3CC(O)OCH_3$		$(CH_3)_3CC(O)OCH_2Cl$		$(CH_3)_3CC(O)OC(O)OH$	
reference	$k_9/k_{reference}$	k_9[a]	$k_{10}/k_{reference}$	k_{10}[a]	$k_{11}/k_{reference}$	k_{11}[a]
C_2H_4	0.44 ± 0.03	4.09 ± 0.28	0.18 ± 0.02	1.67 ± 0.19	0.18 ± 0.02	1.67 ± 0.19
C_2H_5Cl	5.06 ± 0.60	4.07 ± 0.48	2.33 ± 0.10	1.87 ± 0.08	2.01 ± 0.10	1.62 ± 0.08

[a] Units of 10^{-11} cm^3 molecule^{-1} s^{-1}.

$$(CH_3)_3CC(O)OCH_2\bullet + Cl_2 \rightarrow (CH_3)_3CC(O)OCH_2Cl + Cl \quad (14)$$

$$\bullet CH_2(CH_3)_2CC(O)OCH_3 + Cl_2 \rightarrow CH_2Cl(CH_3)_2CC(O)OCH_3 + Cl \quad (15)$$

Unlike $CH_2Cl(CH_3)_2CC(O)OCH_3$, $(CH_3)_3CC(O)OCH_2Cl$ is commercially available and the FTIR system can be calibrated for this species. The yield of $(CH_3)_3CC(O)OCH_2Cl$ provides a measure of the importance of channel (9a). Figure 5 shows a plot of the formation of $(CH_3)_3CC(O)OCH_2Cl$ vs loss of $(CH_3)_3CC(O)OCH_3$ following UV irradiation of $(CH_3)_3CC(O)OCH_3/Cl_2/N_2$ mixtures. Filled symbols are the observed data while the open symbols have been corrected (as described by Meagher et al.[31]) for loss of $(CH_3)_3CC(O)OCH_2Cl$ via reaction with Cl atoms using $k_{10}/k_9 = 0.44$ (see previous section). Linear least-squares analysis of the corrected data in Figure 5 gives a molar $(CH_3)_3CC(O)OCH_2Cl$ yield of 0.11 ± 0.01 (quoted errors are 2 standard deviations). We estimate that systematic uncertainties associated with the calibration of the reference spectra contribute an additional 20% uncertainty. Propagating this additional uncertainty we conclude that $k_{9a}/(k_{9a} + k_{9b}) = 0.11 \pm 0.03$ and, by inference, $k_{9b}/(k_{9a} + k_{9b}) = 0.89 \pm 0.03$.

3.5 Products of the Cl Initiated Oxidation of Methyl Pivalate in the Presence of NO_x. The oxidation of methyl pivalate was studied in the presence of NO. Initial concentrations were 15 mTorr methyl pivalate, 100 mTorr of Cl_2, 9−38 mTorr of NO, 15−600 Torr of O_2 in 700 Torr total pressure of N_2 diluent at 296 K. As discussed above, the reaction of Cl atoms with methyl pivalate in the presence of O_2 leads to the formation of the peroxy radicals $\bullet O_2CH_2(CH_3)_2CC(O)OCH_3$ and $(CH_3)_3CC(O)OCH_2O_2\bullet$ in yields of 89 and 11%, respectively. In the presence of NO, these peroxy radicals react to give the corresponding alkoxy radicals. Information concerning the atmospheric fate of these alkoxy radicals can be derived by studying the products following UV irradiation of methyl pivalate/Cl_2/NO/O_2/N_2 mixtures. Figure 6 shows IR spectra acquired before (A) and after (B) a 45 s UV irradiation of a mixture containing 15.1 mTorr of methyl pivalate, 96 mTorr of Cl_2, and 18 mTorr of NO in 700 Torr of air. Panel C shows the product spectrum obtained after subtraction of features attributable to methyl pivalate from panel B. Comparison of panel C with the reference spectrum of acetone in panel D indicates the formation of acetone. In a similar fashion HCHO, CO, CO_2, and $CH_3OC(O)O_2NO_2$ were also observed as carbon containing products. Figure 7 shows a plot of the observed formation of acetone vs the loss of methyl pivalate following the successive UV irradiation of methyl pivalate/Cl_2/NO/O_2/N_2 mixtures. As seen from Figure 7, independent variation of [NO] over the range 9−38 mTorr and [O_2] over the range 15−600 Torr had no discernible effect on the observed yield of acetone. Linear least-squares analysis of the acetone data in Figure 7 gives a molar yield of 54 ± 4%.

The observation of acetone as product provides important information regarding the atmospheric degradation mechanism of methyl pivalate. As discussed above, 89 ± 3% of the Cl atom attack proceeds at the $(CH_3)_3C-$ group. The resulting peroxy radical will react with NO, such reactions are well-known to proceed via two channels giving an alkoxy radical as the major product and an organic nitrate as the minor product.[32] The resulting alkoxy radical ($\bullet OCH_2(CH_3)_2CC(O)OCH_3$) can either react with O_2 to give an aldehyde or undergo unimolecular decomposition via elimination of HCHO. The observation of an acetone yield of 54 ± 4%, independent of [O_2], shows that the later pathway dominates. Elimination of HCHO produces an alkyl radical which adds O_2 to give a peroxy radical which in turn will react with NO via alkoxy radical and organic nitrate pathways. The alkoxy radical that is formed ($\bullet O(CH_3)_2CC(O)OCH_3$) can isomerize to give a $HO(CH_3)_2CC(O)OCH_2\bullet$ radical, or decompose by elimination of either a CH_3 group to give $CH_3C(O)C(O)OCH_3$, or a $C(O)OCH_3$ fragment to give acetone. The observation of acetone product shows that the later pathway dominates. Using a reference spectrum of $CH_3C(O)C(O)OCH_3$ (methyl pyruvate) an upper limit of 7% for the yield of this species was established. The yield of acetone (54 ± 4%) is significantly less than the fraction of Cl atom attack that proceeds at the $(CH_3)_3C-$ end of the methyl pivalate molecule (89 ± 3%). We attribute this difference to the formation of nitrates in peroxy radical + NO reactions[1,33,34] and isomerization of the $\bullet O(CH_3)_2CC(O)OCH_3$ radical

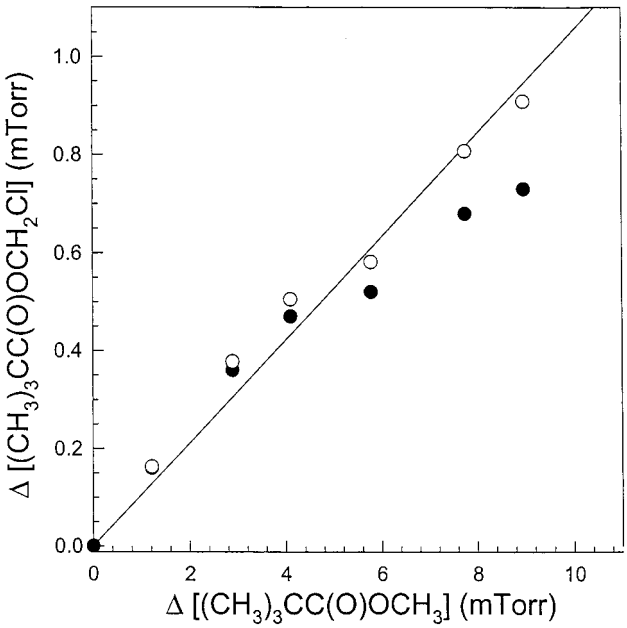

Figure 5. Formation of chloromethyl pivalate vs loss of methyl pivalate following UV irradiation of methyl pivalate/Cl_2/N_2 mixtures (filled symbols are observed data, open symbols have been corrected for secondary reaction with Cl atoms − see text for details).

$$RO_2\bullet + NO \rightarrow RO\bullet + NO_2 \quad (16a)$$

$$RO_2\bullet + NO \rightarrow RONO_2 \quad (16b)$$

Spectroscopic evidence for the formation of organic nitrates was observed in the form of a residual absorption feature at 1662 cm^{-1} which is characteristic of the asymmetric NO_2 stretch in

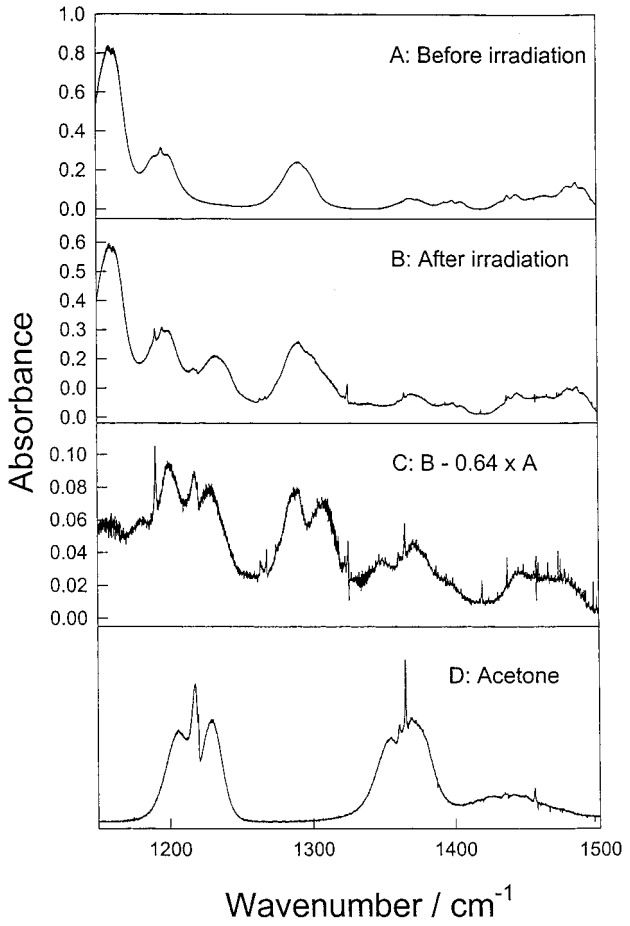

Figure 6. IR spectra before (A) and after (B) a 45 s irradiation of a mixture of 15.1 mTorr of methyl pivalate, 96 mTorr of Cl_2, and 18 mTorr of NO in 700 Torr of air. The consumption of methyl pivalate was 36%. Panel C shows the product spectrum obtained after subtraction of features attributable to methyl pivalate from panel B. Panel D shows the reference spectrum of acetone.

organic nitrates.[35] The yield of $RONO_2$ was unaffected by variation of the [NO] over the range 9−38 mTorr and $[O_2]$ over the range 15−600 Torr showing that under the present experimental conditions the $RONO_2$ product is not formed to any significant degree by addition of NO_2 to the alkoxy radicals. Using an integrated absorption cross section of $(2.5 \pm 0.2) \times 10^{-17}$ cm molecule^{-1} (base 10) for the asymmetric NO_2 stretch[35] gives an estimate of 20 ± 5% for the $RONO_2$ yield. The IR technique is unable to distinguish between the possible organic nitrates formed in the system, and hence, the yield quoted above is an overall yield of organic nitrates in the system.

Thus far, we have not addressed the fate of the peroxy radical generated following Cl atom attack on the $-OCH_3$ end of methyl pivalate. Only 11% of the reaction of Cl atoms with methyl pivalate proceeds at the $-OCH_3$ group. By analogy to the behavior of methyl acetate, we expect 65% of the alkoxy radicals that are formed to undergo α-ester rearrangement and 35% to react with O_2.[36] Hence, we would predict a pivalic acid yield of $11 \times 0.65 = 7\%$ with the remaining 4% giving $(CH_3)_3$-CC(O)OCHO. Using a calibrated reference spectrum of pivalic acid an upper limit of 8% was established for this species. A reference spectrum of $(CH_3)_3CC(O)OCHO$ is not available.

3.6 Products of the OH Initiated Oxidation of Methyl Pivalate in the Presence of NO_x. The products of the OH radical initiated oxidation of methyl pivalate were investigated by the UV irradiation of mixtures of 15 mTorr methyl pivalate, 75−110 mTorr of CH_3ONO, and 7 mTorr of NO in 700 Torr of air diluent at 296 K. The spectral congestion caused by the presence of large concentrations of CH_3ONO in the chamber precluded the observation of any carbon containing products except for acetone. Figure 8 shows a plot of the observed formation of acetone following UV irradiation of methyl pivalate/ CH_3ONO/NO/air mixtures. Linear least-squares analysis gives an acetone yield of 51 ± 6%. It is interesting that the acetone yield measured in the OH radical and Cl atom initiated

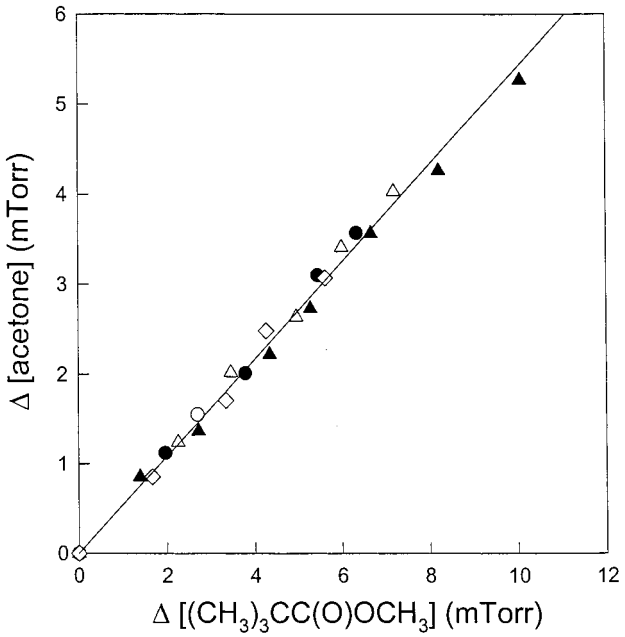

Figure 7. Formation of acetone vs loss of methyl pivalate following UV irradiation of methyl pivalate/Cl_2/NO/O_2/N_2 mixtures. Filled circles show the results using "standard" initial conditions of [methyl pivalate] = 15 mTorr, $[Cl_2]$ = 100 mTorr, [NO] = 18 mTorr, and $[O_2]$ = 147 Torr in 700 Torr total pressure of N_2 diluent at 296 K. Open circles and filled triangles are "standard conditions" but with [NO] decreased to 9, or increased to 38 mTorr, respectively. The open triangles and diamonds are the results obtained using "standard conditions" but with $[O_2]$ decreased to 15, or increased to 600 Torr, respectively.

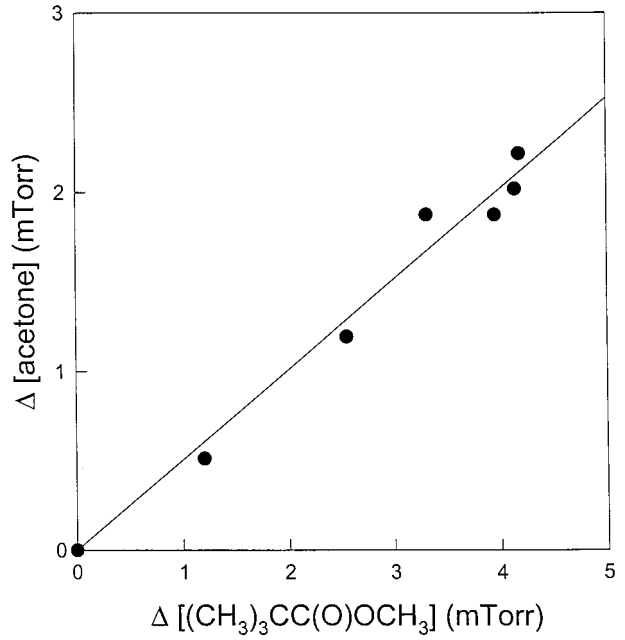

Figure 8. Formation of acetone vs loss of methyl pivalate following UV irradiation of methyl pivalate/CH_3ONO/NO/O_2/N_2 mixtures in 700 Torr of air at 296 K.

TABLE 3: Atmospheric Oxidation Mechanism for Methyl Pivalate in the Presence of NO_x

	reaction[a]	notes[b]	branching[c] rxn (%)	branching[c] total (%)
	$CH_3C(CH_3)(CH_3)C(O)OCH_3$			
1b	$+ OH \rightarrow H_2O + CH_3C(CH_3)(CH_2\bullet)C(O)OCH_3$	1	75	75
1a	$+ OH \rightarrow H_2O + CH_3C(CH_3)(CH_3)C(O)OCH_2\bullet$		25	25
	radicals formed from reaction at tert-butyl end			
3	$CH_3C(CH_3)(CH_2\bullet)C(O)OCH_3 + O_2 \rightarrow CH_3C(CH_3)(CH_2OO\bullet)C(O)OCH_3$			75
	$CH_3C(CH_3)(CH_2OO\bullet)C(O)OCH_3$			
17	$+ NO \rightarrow$ **$CH_3OC(O)C(CH_3)(CH_3)CH_2ONO_2$**	2	13	10
18	$+ NO \rightarrow NO_2 + CH_3C(CH_3)(CH_2O\bullet)C(O)OCH_3$		87	65
	$CH_3C(CH_3)(CH_2O\bullet)C(O)OCH_3$			
19	$+ O_2 \rightarrow$ **$CH_3C(CH_3)(CHO)C(O)OCH_3 + HO_2\bullet$**	3	5	3
20	$\rightarrow$ **HCHO** $+ CH_3C(\bullet)(CH_3)C(O)OCH_3$	4	95	62
21	$CH_3C(\bullet)(CH_3)C(O)OCH_3 + O_2 \rightarrow CH_3C(OO\bullet)(CH_3)C(O)OCH_3$			62
	$CH_3C(OO\bullet)(CH_3)C(O)OCH_3$			
22	$+ NO \rightarrow$ **$CH_3C(CH_3)(ONO_2)C(O)OCH_3$**	5	6	4
23	$+ NO \rightarrow NO_2 + CH_3C(O\bullet)(CH_3)C(O)OCH_3$		94	58
	$CH_3C(O\bullet)(CH_3)C(O)OCH_3$			
24	$\rightarrow$ **$CH_3C(O)CH_3$** $+ CH_3OC(O)\bullet$	6	86	50
25	$\rightarrow CH_3C(CH_3)(OH)C(O)OCH_2\bullet$	7	14	8
26	$CH_3{-}OC(O)\bullet + O_2 \rightarrow CH_3OC(O)OO\bullet$			50
27	$CH_3C(CH_3)(OH)C(O)OCH_2\bullet + O_2 \rightarrow CH_3C(CH_3)(OH)C(O)OCH_2OO\bullet$			8
28	$CH_3C(CH_3)(OH)C(O)OCH_2OO\bullet + NO \rightarrow NO_2 + CH_3C(CH_3)(OH)C(O)OCH_2O\bullet$			8
	$CH_3C(CH_3)(OH)C(O)OCH_2O\bullet$			
29	$+ O_2 \rightarrow$ **$CH_3C(CH_3)(OH)C(O)OCHO + HO_2\bullet$**	8	34	3
30	$\rightarrow$ **$CH_3C(CH_3)(OH)C(O)OH$** $+ HCO\bullet$	9	66	5
31	$HCO\bullet + O_2 \rightarrow CO + HO_2\bullet$			19
	radicals formed from reaction at methoxy end			
2	$CH_3C(CH_3)(CH_3)C(O)OCH_2\bullet + O_2 \rightarrow CH_3C(CH_3)(CH_3)C(O)OCH_2OO\bullet$			25
	$CH_3C(CH_3)(CH_3)C(O)OCH_2OO\bullet$			
32	$+ NO \rightarrow$ **$CH_3C(CH_3)(CH_3)C(O)OCH_2ONO_2$**	2	13	3
33	$+ NO \rightarrow NO_2 + CH_3C(CH_3)(CH_3)C(O)OCH_2O\bullet$		87	22
	$CH_3C(CH_3)(CH_3)C(O)OCH_2O\bullet$			
34	$+ O_2 \rightarrow$ **$CH_3C(CH_3)(CH_3)C(O)OCHO + HO_2\bullet$**	8	34	7
35	$\rightarrow$ **$CH_3C(CH_3)(CH_3)C(O)OH$** $+ HCO\bullet$	9	66	14

[a] Predicted stable organic products are shown in bold font. [b] Documentation notes for branching ratios are as follows. See Carter[18] for details concerning the estimates of the alkoxy radical reactions. 1 This work (see section 3.7). 2 This work (see section 3.8). 3 Estimated rate constant for reaction with O_2 is 6.0×10^{-14} exp(-0.63 kcal mol^{-1}/RT) $= 2.08 \times 10^{-14}$ cm^3 molecule^{-1} s^{-1} at 300 K. 4 Estimated decomposition rate constant is 2.0×10^{14} exp(-10.99 kcal mol^{-1}/RT) $= 1.96 \times 10^6$ s^{-1} at 300 K. 5 Nitrate yield adjusted to fit environmental chamber reactivity data for methyl isobutyrate.[18] 6 Estimated decomposition rate constant is 2.0×10^{14} exp(-14.50 kcal mol^{-1}/RT) $= 5.44 \times 10^3$ s^{-1} at 300 K. 7 Rate constant for 1,4-H-shift isomerization is estimated to be 2.4×10^{11} exp(-8.49 kcal mol^{-1}/RT) $= 8.97 \times 10^2$ s^{-1} at 300 K. 8 Estimated rate constant for reaction with O_2 is 6.0×10^{-14} exp(-1.45 kcal mol^{-1}/RT) $= 5.27 \times 10^{-15}$ cm^3 molecule^{-1} s^{-1} at 300 K. 9 The rate constant for the ester rearrangement reaction is estimated to be 8.0×10^{10} exp(-8.49 kcal mol^{-1}/RT) $= 5.24 \times 10^4$ s^{-1} at 300 K. [c] Predicted branching ratios. The "Rxn" column shows the importance of the reaction relative to the competing reactions of the species or radical. The "Total" column show the importance of the reaction relative to the overall process.

experiments is indistinguishable. This suggests that as was the case for Cl atom attack, the reaction of OH radicals with methyl pivalate proceeds mainly at the $(CH_3)_3C-$ group. Taking the ratio of observed acetone yields, the measured value of $k_{9b}/(k_{9a} + k_{9b}) = 0.89 \pm 0.03$, and assuming that attack on the $-OCH_3$ end of methyl pivalate does not lead to acetone formation we can estimate that $k_{1b}/(k_{1a} + k_{1b}) = (0.89 \pm 0.03) \times (0.51 \pm 0.06)/(0.54 \pm 0.04) = 0.84 \pm 0.12$, and, by inference, $k_{1a}/(k_{1a} + k_{1b}) = 0.16 \pm 0.12$. This estimate is consistent with the conclusions presented in section 3.1.

3.7 Mechanism of the OH Initiated Atmospheric Oxidation of Methyl Pivalate. Table 3 shows the detailed mechanism describing the OH initiated oxidation of methyl pivalate under atmospheric conditions in the presence of NO_x derived in the present work. This mechanism is based upon the results presented above with estimation methods used to assess the relative importance of competing reactions of alkoxy and peroxy radicals. Table 3 lists the estimated branching ratios and overall importance of competing processes. The footnotes to Table 3 indicate how the branching ratios were derived.

The branching ratio for the reaction of OH radicals with methyl pivalate can be estimated using the group additivity method of Kwok and Atkinson.[37] This method predicts $k_{1b}/(k_{1a} + k_{1b}) = 0.7$ and an overall rate constant $k_1 = 7.34 \times 10^{-13}$ cm^3 molecule^{-1} s^{-1}. The value of k_1 predicted by the group additivity method is a factor of 1.6 lower than that which we measure experimentally (see section 3.1). We conclude that the group additivity method under-estimates either k_{1a}, or k_{1b}, or both. Interestingly, use of the branching ratio $k_{1b}/(k_{1a} + k_{1b}) = 0.7$ estimated by the group additivity method gives a predicted acetone yield of 46%, which is only slightly lower than the measured value of 51%. We choose to adopt a branching ratio $k_{1b}/(k_{1a} + k_{1b}) = 0.75$, so that the 51% acetone yield is predicted more closely. This is well within the uncertainty of the branching ratio estimate.

Under conditions where NO_x is present and O_3 formation occurs, the fate of peroxy radicals is reaction with NO giving NO_2 and alkoxy radicals as major products and alkyl nitrates as minor product (see reaction 16). Consistent with the $20 \pm 5\%$ overall nitrate yield estimated from the IR data (see section 3.5) it was found that assuming an overall nitrate yields of $\sim$18% gives the best model predictions of the ozone reactivity in environmental chamber data (see section 3.8). Allowing for the sequential formation of peroxy radicals in the multistep mechanism, this gives about a 9% nitrate formation branching ratio in the reactions of NO with the initially formed peroxy

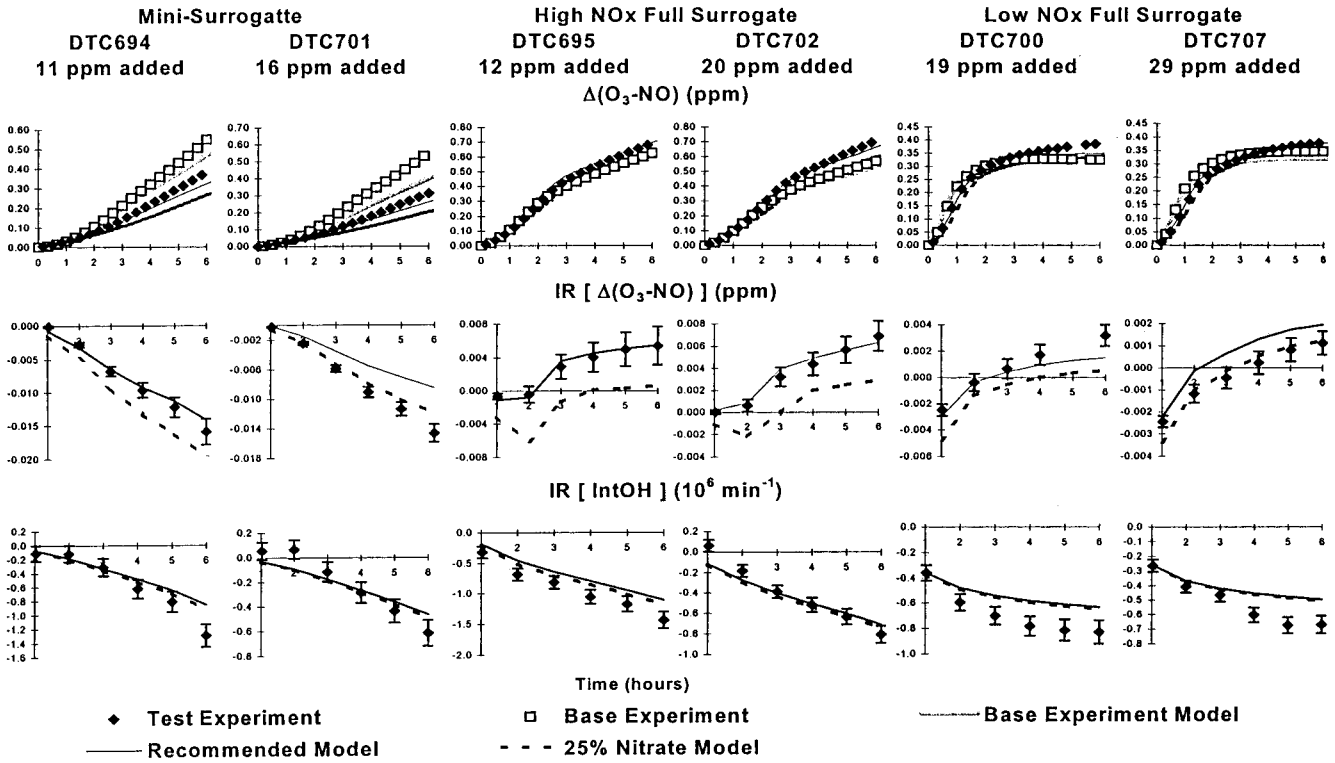

Figure 9. Experimental and calculated concentration time plots for $\Delta([O_3] - [NO])$ and incremental reactivities relative to $\Delta([O_3] - [NO])$ and IntOH for the environmental chamber reactivity experiments.

radicals in the methyl pivalate reaction. This is very close to the estimate of Carter[18] of ~10% nitrate yields in these reactions, based on the nitrate yields needed to fit model simulations to environmental chamber data for other compounds.

Formaldehyde, acetone, organic nitrate, and $CH_3OC(O)\bullet$ radicals are predicted to be the major products following OH attack at the *tert*-butyl group. Formation of ~3% $CH_3C(CH_3)(CHO)C(O)OCH_3$ is predicted from the minor reaction of O_2 with the initially formed peroxy radical, and formation of ~3% $CH_3C(CH_3)(OH)C(O)OCHO$ and ~5% $CH_3C(CH_3)(OH)C(O)OH$ is predicted following the isomerization of the $CH_3C(O\bullet)(CH_3)C(O)OCH_3$ radical, which competes with the decomposition forming acetone. Although these products were not detected, the data obtained in this study does not rule out their formation in small yields.

In terms of model species used in the SAPRC-99 mechanism,[18] the overall process for the reactions shown in Table 3 can be represented as follows:

OH + Methyl Pivalate → 0.317 RO2−R• + 0.176 RO2−N• + 1.221 R2O2• + 0.507 RCO−O2• + 0.187 CO + 0.631 HCHO + 0.034 RCHO + 0.507 ACET + 0.096 MEK + 0.187 RCO−OH

RO2−R• represents peroxy radicals that react to convert NO to NO_2 and form HO_2. RO2−N• represents peroxy radicals that react with NO to form organic nitrates. R2O2• represents extra NO to NO_2 conversions caused by peroxy radicals formed in multistep mechanisms. RCO−O2• represents the lumped higher acyl peroxy radical (used for $CH_3OC(O)OO\bullet$ in this case). HCHO represents formaldehyde. RCHO represents the aldehyde $CH_3C(CH_3)(CHO)C(O)OCH_3$. ACET represents acetone. MEK represents the lumped lower reactivity oxygenated products $CH_3C(CH_3)(CH_3)C(O)OCHO$ and $CH_3C(CH_3)(OH)C(O)OCHO$. Finally, RCO−OH represents the lumped higher organic acid $CH_3C(CH_3)(CH_3)C(O)OH$ and $CH_3C(CH_3)(OH)C(O)OH$. This mechanism was used in the model simulations discussed in the following section. The overall rate constant used was $k_1 = 1.18 \times 10^{-12}$ cm^3 molecule^{-1} s^{-1}, based on the 298K measurement made in this work.

3.8 Results of Ozone Reactivity Environmental Chamber Experiments. Six dual-chamber incremental reactivity experiments were carried out for this program, two with each of the three kinds of base case ROG−NO_x systems. Concentration time plots for $\Delta([O_3] - [NO])$ data and the incremental reactivities relative to $\Delta([O_3] - [NO])$ and IntOH are shown in Figure 9. Figure 10 shows concentration time plots for the two organic compounds monitored, formaldehyde and acetone. Note that formaldehyde is formed in the base case experiments but acetone is not. Because of its relatively low rate of reaction, extremely large amounts of methyl pivalate had to be added in these experiments to have a measurable effect on the results (10−30 ppm of methyl pivalate vs. 4−6 ppmC of base ROG mixture).

Figure 9 shows that methyl pivalate has a negative effect on rates of NO oxidation and O_3 formation in the mini-surrogate experiments and has negative or small effects in the beginning of the full surrogate experiments, but has positive effects on O_3 at the end of the full surrogate runs. It also has negative effects on OH radical levels in all experiments. The negative effect of methyl pivalate on radical levels is ascribed to radical termination due to nitrate formation in the RO_2 + NO reactions, and $CH_3OC(O)OONO_2$ formation. This slows down the reactions of all reactive organics present and thereby inhibits NO oxidation and O_3 formation. However, methyl pivalate's reactions also convert NO to NO_2, which has a positive effect on NO oxidation and O_3 formation rates. The mini-surrogate experiments are relatively more sensitive to radical inhibition effects compared to direct NO to NO_2 conversions so the overall effect on $\Delta([O_3] - [NO])$ is negative. The full surrogate experiments are less sensitive to radical inhibition effects than to direct NO to NO_2 conversions,[6] and in the case of methyl pivalate the net effect on $\Delta([O_3] - [NO])$ is positive.

As shown in Figure 10, the addition of methyl pivalate causes measurable acetone formation in all experiments. The mecha-

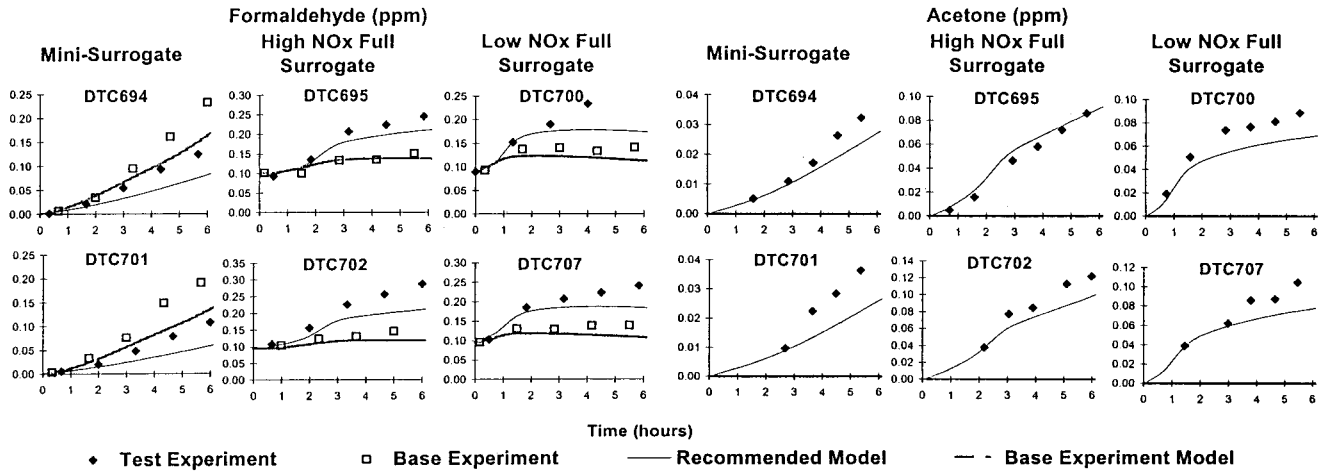

Figure 10. Experimental and calculated concentration time plots for formaldehyde and acetone for the environmental chamber reactivity experiments.

nism predicts that formaldehyde is a coproduct with methyl pivalate, and consistent with this the methyl pivalate causes an increase in the formaldehyde yields in the full surrogate runs. However, the methyl pivalate causes formaldehyde to decrease in the mini-surrogate runs. This is because the radical inhibition caused by methyl pivalate, which is relatively more important in the mini-surrogate experiments, decreases the rate of formaldehyde formation from the ethene in the base case mixture.

3.9 Results of Mechanism Evaluation Using Ozone Reactivity Chamber Experiments. Figure 9 shows the results of the model simulations of the methyl pivalate reactivity results using the SAPRC-99 mechanism with the methyl pivalate mechanism given in Table 3. The recommended mechanism fits all the chamber data well except for run DTC701, where the reactivity predictions are considered to be less reliable because the mechanism does not simulate the base case experiment particularly well (the mini-surrogate experiments tend to be sensitive to uncertainties and variations in the chamber radical source[5]). Fits to the low NO_x full surrogate runs are not quite as good as those to the higher NO_x runs, but no consistent biases are seen except for a tendency to under predict the inhibition of IntOH reactivities. However, as discussed elsewhere,[6,8] inhibitions of IntOH reactivities in the low NO_x experiments tend to be under predicted for almost all VOCs, suggesting a problem with the overall base mechanism under low NO_x conditions. Figure 10 shows that the model gives reasonably good predictions of the qualitative effects of methyl pivalate on formaldehyde and acetone formation, though it has a slight bias toward under predicting their yields in some experiments. Considering the overall performance of the model in simulating reactivity data for compounds with known mechanisms[5,14,18,38] the fits shown in Figures 9 and 10 are good.

The fits of the model simulations of the reactivity data shown in Figure 9 were obtained after adjusting the nitrate yields in the reactions of RO_2 with NO to minimize the biases in the model simulations to the data. The model predictions are sensitive to this parameter. To illustrate this sensitivity, the dotted lines in Figure 9 show results obtained using a 25% overall nitrate yield (upper extreme of experimental range given in section 3.5) instead of the best fit ~18% yield. Assuming higher nitrate yields causes significantly lower predicted $\Delta([O_3] - [NO])$ reactivities in the higher NO_x full surrogate experiments and causes a bias toward under predicting it in the lower NO_x full surrogate runs and in the mini-surrogate experiment where the model gives the better fit to the base case experiment.

4. Implications for Atmospheric Chemistry

We report here a large body of experimental and modeling data which improve our understanding of the atmospheric chemistry of methyl pivalate. Photolysis is a negligible atmospheric loss mechanism for methyl pivalate. At a temperature of 270 K (appropriate for evaluation of atmospheric lifetimes with respect to reaction with OH[39]) hydroxyl radicals react 214 ($1.24 \times 10^{-12}/5.8 \times 10^{-15}$) times faster with methyl pivalate than with methyl chloroform. Methyl chloroform has an atmospheric lifetime of 5.9 years with respect to reaction with OH radicals. Hence, the atmospheric lifetime of methyl pivalate can be estimated to be approximately 10 days.

The data obtained in this work were used to formulate a detailed mechanism (see Table 3) describing the atmospheric oxidation of methyl pivalate. This mechanism was found to give predictions of the effects of methyl pivalate on O_3 formation and other measures of reactivity that are in good agreement with results of environmental chamber experiments. We recommend that this mechanism be used in future airshed models to predict the effects of methyl pivalate emissions on air quality.

Finally, it is of interest to consider the potential impact of the atmospheric oxidation of methyl pivalate on the global acetone budget. The global source strength of acetone is approximately 50 Tg per year[40] (1 Tg = 10^{12} g). If methyl pivalate finds large scale industrial use it is likely to be produced at a level of 0.01−0.10 Tg per year. Methyl pivalate oxidation gives acetone in a 20% mass yield. Assuming an industrial production of 0.10 Tg and 100% release, the atmospheric oxidation of methyl pivalate would perturb the global atmospheric acetone budget by < 0.04%.

Acknowledgment. We thank Peter Ellis (ExxonMobil Chemical Company) for his help and advice during the course of this work.

References and Notes

(1) Tyndall, G. S.; Cox, R. A.; Granier, C.; Lesclaux, R.; Moortgat, G. K.; Pilling, M. J.; Ravishankara, A. R.; Wallington, T. J. *J. Geophys. Res.* **2000**, in press.

(2) Orkin, V. L.; Huie, R. E.; Kurylo, M. J. *J. Phys. Chem.* **1996**, *100*, 8907.

(3) Orkin, V. L.; Huie, R. E.; Kurylo, M. J. *J. Phys. Chem.* **1997**, *101*, 9118.

(4) Wallington, T. J.; Japar, S. M. *J. Atmos. Chem.* **1989**, *9*, 399.

(5) Carter, W. P. L.; Pierce, J. A.; Luo, D.; Malkina, I. L. *Atmos. Environ.* **1995**, *29*, 2499.

(6) Carter, W. P. L.; Luo, D.; Malkina, I. L.; Pierce, J. A., "Environmental Chamber Studies of Atmospheric Reactivities of Volatile Organic

Compounds. Effects of Varying ROG Surrogate and NOx," Final report to Coordinating Research Council, Inc., Project ME−9, California Air Resources Board, Contract A032-0692, and South Coast Air Quality Management District, Contract C91323. March 24, 1995. Available at http://www.cert.ucr.edu/∼carter/absts.htm#rct2rept.

(7) Carter, W. P. L.; Luo, D.; Malkina, I. L., "Environmental Chamber Studies for Development of an Updated Photochemical Mechanism for VOC Reactivity Assessment," Final report to the California Air Resources Board, the Coordinating Research Council, and the National Renewable Energy Laboratory, November 26, 1997. Available at http://www.cert.ucr.edu/∼carter/absts.htm#rct3rept.

(8) Carter, W. P. L.; Luo, D.; Malkina, I. L., "Investigation of Atmospheric Reactivities of Selected Consumer Product VOCs," Report to California Air Resources Board, May 30, 2000. Available at http://www.cert.ucr.edu/∼carter/absts. htm#cpreport.

(9) Carter, W. P. L.; Luo, D.; Malkina, I. L.; Fitz, D., "The University of California, Riverside Environmental Chamber Data Base for Evaluating Oxidant Mechanism. Indoor Chamber Experiments through 1993," Report submitted to the, U. S. Environmental Protection Agency, EPA/AREAL, Research Triangle Park, NC.; March 20, 1995. Available at http://www.cert.ucr.edu/∼carter/absts.htm#databas.

(10) Zafonte, L.; Rieger, P. L.; Holmes, J. R. *Environ. Sci. Technol.* **1977**, *11*, 483−487.

(11) Dasgupta, P. K.; Dong, S.; Hwang, H. *Atmos. Environ*. **1988**, *22*, 949.

(12) Dasgupta, P. K.; Dong, S.; Hwang, H. *Aerosol Sci. Tech.* **1990**, *12*, 98.

(13) Johnson, G. M. "Factors Affecting Oxidant Formation in Sydney Air," In *The Urban Atmosphere—Sydney, A Case Study*; Carras, J. N., Johnson, G. M., Eds.; CSIRO: Melbourne, 1983, pp 393−408.

(14) Carter, W. P. L.; Atkinson, R. *Environ. Sci. Technol*. **1987**, *21*, 670.

(15) Carter, W. P. L.; Lurmann, F. W. *Atmos. Env*iron. **1991**, *25A*, 2771.

(16) Carter, W. P. L. *Atmos. Environ* **29**, 2513, 1995.

(17) Atkinson, R. *J. Phys. Chem. Ref. Data* **1989**, Monograph no 1.

(18) Carter, W. P. L., "Documentation of the SAPRC-99 Chemical Mechanism for VOC Reactivity Assessment," Report to the California Air Resources Board, Contracts 92−329 and 95−308, May 8, 2000. Available at http://www.cert.ucr.edu/∼carter/absts.htm#saprc99.

(19) Carter, W. P. L.; Atkinson, R.; Winer, A. M.; Pitts, J. N., Jr. *Int. J. Chem. Kinet*. **1982**, *14*, 1071.

(20) DeMore, W. B.; Sander, S. P.; Golden, D. M.; Hampson, R. F.; Kurylo, M. J.; Howard, C. J.; Ravishankara, A. R.; Kolb, C. E.; Molina, M. J. *Chemical Kinetics and Photochemical Data for Use in Stratospheric Modeling, Evaluation No. 12*; JPL Publication 97-4. Jet Propulsion Laboratory, California Institute of Technology: Pasadena, CA, 1997.

(21) Dagaut, P.; Wallington, T. J.; Liu, R.; Kurylo, M. J. *Int. J. Chem. Kinet.* **1988**, *20*, 331.

(22) Wallington, T. J.; Kurylo, M. J. *J. Phys. Chem.* **1987**, *91*, 5050.

(23) Bilde, M.; Møgelberg, T. E.; Sehested, J.; Nielsen, O. J.; Wallington, T. J.; Hurley, M. D.; Japar, S. M.; Dill, M.; Orkin, V. L.; Buckley, T. J.; Huie, R. E.; Kurylo, M. J. *J. Phys. Chem.* **1997**, *101*, 3514.

(24) Wallington, T. J.; Dagaut, P.; Liu, R.; Kurylo, M. J. *Int. J. Chem. Kinet.* **1988**, *20*, 177.

(25) El Boudali, A.; Le Calve, S.; Le Bras, G.; Mellouki, A. *J. Phys. Chem.* **1996**, *100*, 12 364.

(26) Wollenhaupt, M.; Carl, S. A.; Horowitz, A.; Crowley, J. N. *J. Phys. Chem. A* **2000**, *104*, 2695.

(27) Le Calvé, S.; Hitier, D.; Le Bras, G.; Mellouki, A. *J. Phys. Chem. A* **1998**, *102*, 4579.

(28) Calvert, J. G.; Pitts, N. J., Jr. *Photochemistry*; John Wiley and Sons Inc.: New York, 1967.

(29) Wallington, T. J.; Andino, J. M.; Lorkovic, I. M.; Kaiser, E. W.; Marston, G. *J. Phys. Chem.* **1990**, *94*, 3644.

(30) Wine, P. H.; Semmes, D. H. *J. Phys. Chem.* **1983**, *87*, 3572.

(31) Meagher, R. J.; McIntosh, M. E.; Hurley, M. D.; Wallington, T. J. *Int. J. Chem. Kinet.* **1997**, *29*, 619.

(32) Wallington, T. J.; Dagaut, P.; Kurylo, M. J. *Chem. Rev*. **1992**, *92*, 667.

(33) Becker, K. H.; Geiger, H.; Wiesen, P. *Chem. Phys. Lett*. **1991**, *184*, 256.

(34) Atkinson, R.; Aschmann, S. M.; Carter, W. P. L.; Winer, A. M.; Pitts, J. N., Jr., *J. Phys. Chem*. **1982**, *86*, 4563.

(35) Tuazon, E. C.; Aschmann, S.; M.; Atkinson, R. *Environ. Sci. Tech.* **1999**, *33*, 2885.

(36) Christensen, L.; Ball, J. C.; Wallington, T. J. *J. Phys. Chem. A.* **2000**, *104*, 345.

(37) Kwok, E. S. C.; Atkinson, R. *Atmos. Environ.* **1995**, *29*, 1685.

(38) Carter, W. P. L.; Lurmann, F. W. *Atmos. Environ*. **1991**, *25A*, 2771.

(39) Spivakovsky, C. M.; Logan, J. A.; Montzka, S. A.; Balkanski, Y. J.; Foreman-Fowler, M.; Jones, D. B. A.; Horowitz, L. W.; Fusco, A. C.; Brenninkmeijer, C. A. M.; Prather, M. J.; Wofsy, S. C.; McElroy, M. B. *J. Geophys. Res.* **2000**, *105*, 8931.

(40) Singh, H. B.; O'Hara, D.; Herlth, D.; Sachse, W.; Blake, D. R.; Bradshaw, J. D.; Kanakidou, M.; Crutzen, P. J. *J. Geophys. Res.* **1994**, *99*, 1805.